

# Understanding the Dynamics of Glass-forming Liquids with Random Pinning within the Random First Order Transition Theory

Saurish Chakrabarty<sup>1,2,\*</sup>, Rajsekhar Das<sup>3,†</sup>, Smarajit Karmakar<sup>3,‡</sup> and Chandan Dasgupta<sup>2,4,§</sup>

<sup>1</sup> *International Centre for Theoretical Sciences, Tata Institute of Fundamental Research, Shivakote, Hesaraghatta, Hubli, Bangalore, 560089, India,*

<sup>2</sup> *Centre for Condensed Matter Theory, Department of Physics, Indian Institute of Science, Bangalore, 560012, India,*

<sup>3</sup> *Centre for Interdisciplinary Sciences, Tata Institute of Fundamental Research, 21 Brundavan Colony, Narisingi, Hyderabad, India,*

<sup>4</sup> *Jawaharlal Nehru Centre for Advanced Scientific Research, Bangalore 560064, India.*

Extensive computer simulations are performed for a few model glass-forming liquids in both two and three dimensions to study their dynamics when a randomly chosen fraction of particles are frozen in their equilibrium positions. For all the studied systems, we find that the temperature-dependence of the  $\alpha$  relaxation time extracted from an overlap function related to the self part of the density autocorrelation function can be explained within the framework of the Random First Order Transition (RFOT) theory of the glass transition. We propose a scaling description to rationalize the simulation results and show that our data for the  $\alpha$  relaxation time for all temperatures and pin concentrations are consistent with this description. We find that the fragility parameter obtained from fits of the temperature dependence of the  $\alpha$  relaxation time to the Vogel-Fulcher-Tammann (VFT) form decreases by almost an order of magnitude as the pin concentration is increased from zero. Our scaling description relates the fragility parameter to the static length scale of RFOT and thus provides a physical understanding of fragility within the framework of the RFOT theory. Implications of these findings for the values of the exponents appearing in the RFOT theory are discussed.

## I. INTRODUCTION

The rapid rise of the viscosity of glass forming liquids with decreasing temperature remains one of the important unsolved problems in condensed matter physics [1–8]. In the Random First Order Transition (RFOT) theory [9–11], the growth of the viscosity is attributed to an *ideal glass transition* at which the configurational entropy associated with the multiplicity of amorphous minima of the free energy goes to zero. This transition is supposed to take place at the Kauzmann temperature  $T_K$  at which the excess entropy of a supercooled liquid extrapolates to zero. This temperature is found to be close to  $T_{VFT}$ , the temperature at which a Vogel-Fulcher-Tammann (VFT) fit to temperature dependence of the viscosity of a fragile glass-forming liquid predicts a divergence of the viscosity. Equilibrium and dynamical properties of liquids near  $T_{VFT} \simeq T_K$  can not be studied in experiments or computer simulations because liquids fall out of equilibrium at substantially higher temperatures. For this reason, the occurrence of the ideal glass transition of RFOT theory remains controversial.

The kinetic fragility [12], which measures the rate at which the viscosity increases with decreasing temperature, is another interesting but poorly understood aspect of the dynamics near the glass transition. The micro-

scopic origin of fragility has been investigated in many numerical studies [13–17]. In these studies, attempts were made to tune the fragility by changing different parameters of the system, *e.g.* the degree of polydispersity in particle size [13], softness of the pair potential [16], the density of a system of particles interacting via a Hertzian potential [15], the composition of binary glass-forming liquids [14], and the height of a narrow repulsive spike in the pair potential [17]. In some of these cases [13, 16], the fragility was found to depend weakly on the tuning parameters, so that no clear conclusion about the origin of fragility could be reached. On the other hand, in Refs. [14, 15, 17], the fragility was found to change by substantial amounts and correlations of the fragility with other thermodynamic quantities were obtained. However, a clear understanding of the microscopic origin of fragility remains elusive.

Recently, it has been proposed [18] that the ideal glass transition of RFOT may be accessible in experiments and simulations of systems in which a randomly chosen fraction of the constituent particles are pinned at their positions in an equilibrium configuration of the liquid. It is argued [18] that the temperature  $T_K$  at which the configurational entropy goes to zero in such a system increases as the concentration of pinned particles is increased, thereby making it possible to equilibrate the liquid near the higher transition temperature. Results of numerical studies [19, 20, 22] of equilibrium properties of such randomly pinned systems are consistent with the predictions of Ref. [18]. On the other hand, a numerical study [21] of the dynamics of two model liquids with random pinning indicates that the VFT temperature  $T_{VFT}$

\*Electronic address: saurish@icts.res.in

†Electronic address: rajsekhard@tifrh.res.in

‡Electronic address: smarajit@tifrh.res.in

§Electronic address: cdgupta@physics.iisc.ernet.in

obtained from the temperature-dependence of the  $\alpha$  relaxation time extracted from the self part of the intermediate scattering function or a related overlap function remains constant or decreases slightly with increasing pin concentration. It is also shown in Ref. [21, 23] that the  $\alpha$  relaxation time defined there remains finite at temperatures close to the values at which the equilibrium calculation of Ref. [22] predicts a vanishing of the configurational entropy. These results raise important questions about the validity of the relation between the configurational entropy and the  $\alpha$  relaxation time predicted in RFOT theory. Possible explanations of this discrepancy have been suggested [23, 24], but a clear resolution is not yet available.

In Ref. [21], it was also shown that the fragility can be tuned very effectively by changing the fraction of pinned particles. Pinning decreases the kinetic fragility and by increasing the concentration of pinned particles, one can change the fragility by a large factor ( $\simeq 10$ ), comparable to experimentally observed variations of the fragility in different glass forming liquids. Thus, random pinning provides a nice way of tuning the fragility without changing the microscopic details of the system. Recently, random pinning of the kind considered here has been realized experimentally [25] in two-dimensional colloidal systems. This suggests that it will not be difficult to tune the fragility in experimental colloidal glasses in the near future. It is, therefore, important to understand the reason for the variation of the fragility seen [21] in the dynamics of randomly pinned liquids.

To address some of the outstanding questions mentioned above, we have carried out detailed molecular dynamics simulations of four models of glass-forming liquids with random pinning. These models include the three-dimensional models considered in our earlier study [21] and two two-dimensional models. The dependence of the  $\alpha$ -relaxation time, obtained from an overlap function analogous to the self part of the density autocorrelation function, on the temperature and the pin concentration in the two-dimensional models is found to be qualitatively similar to that in three dimensions. It was suggested in Ref. [24] that the relaxation time extracted from the *full* density autocorrelation function should be considered in a check of whether the relaxation time diverges at the points at which the configurational entropy vanishes according to the numerical results of Ref. [22]. We have calculated the autocorrelation function of the full density in one of the three-dimensional models (the Kob-Andersen model [26] which was also considered in Ref. [22]) and found that the time scale associated with the decay of this function is actually *smaller* than that of the time scale extracted from the overlap function. Thus, considering the autocorrelation function of the full density does not resolve the discrepancy between the behavior of the relaxation time and the results for the configurational entropy reported in Ref. [22].

We show that an alternative description proposed in Ref. [21], based on the assumption that the configura-

tional entropy of the pinned system differs from that of the unpinned system by a multiplicative factor that decreases from unity as the concentration of pinned particles is increased from zero, allows us to reconcile the results for the dynamics, as well as new results for the configurational entropy of the unpinned systems, with the RFOT theory. This assumption leads to a scaling description [21] of the dynamics that involves a new static length scale  $\xi_p$  associated with the effect of random pinning on the  $\alpha$  relaxation time. We show that our data for the relaxation time for all temperatures and pin concentrations considered in our study are consistent with this scaling description. The relation between the pinning length scale  $\xi_p$  and the static length scale  $\xi_s$  of RFOT theory is studied in detail. This allows us to estimate the values of the exponent  $\theta$ , associated with the dependence of the interface free energy on the system size, and the exponent  $\psi$  that describes the dependence of the time scale on  $\xi_s$  in the RFOT theory. We find that  $\theta \simeq d-1$  ( $d$  is the spatial dimension),  $\psi \simeq 1$  for the three-dimensional models considered here. In one of the two-dimensional models studied here, we find that  $\theta \simeq d-1$ ,  $\psi \simeq 0.7$ , whereas the value of  $\theta$  estimated for the other two-dimensional model does not satisfy the bound  $\theta \leq d-1$ . We also find that the static length scale of the RFOT theory is intimately connected to the fragility, thereby providing a rationale for the variation of fragility in different glass forming liquids.

The rest of the paper is organized as follows. First, we define the models studied here and describe the methods used in our simulations and calculations of quantities of interest. After a brief review of the predictions of the RFOT theory for the relationships among different dynamic and thermodynamic quantities, such as the relaxation time ( $\tau_\alpha$ ), the static length scale ( $\xi_s$ ) and the configurational entropy density ( $s_c$ ), we present our numerical results and their analysis within the framework of the RFOT theory using the scaling description proposed in Ref. [21]. The main results of the scaling analysis for the exponents appearing in the RFOT theory and the microscopic origin of the fragility parameter are discussed. We close with a summary of the main conclusions and their implications for the validity of the RFOT theory.

## II. MODELS AND METHODS

**Models:** We have studied four different model glass forming liquids in this study – two models each in two and three dimensions. The first model glass former we study is the well-known Kob- Andersen 80:20 binary Lennard-Jones mixture in three dimensions. Here it is referred to as the **3dKA model**. The interaction potential in this model is given by

$$V_{\alpha\beta}(r) = 4\epsilon_{\alpha\beta} \left[ \left( \frac{\sigma_{\alpha\beta}}{r} \right)^{12} - \left( \frac{\sigma_{\alpha\beta}}{r} \right)^6 \right], \quad (1)$$

where  $\alpha, \beta \in \{A, B\}$  and  $\epsilon_{AA} = 1.0$ ,  $\epsilon_{AB} = 1.5$ ,  $\epsilon_{BB} = 0.5$ ,  $\sigma_{AA} = 1.0$ ,  $\sigma_{AB} = 0.80$ ,  $\sigma_{BB} = 0.88$ . The interaction potential is cut off at  $2.50\sigma_{\alpha\beta}$  and we use a quadratic polynomial to make the potential and its first two derivatives smooth at the cutoff distance. The temperature range studied for this model is  $T \in [0.45, 3.00]$  at number density  $\rho = 1.20$ . The same model with 65:35 composition is used in the two dimensional simulations. We refer to this model as the **2dMKA model**. The 65:35 composition is chosen to make sure that the system does not show any crystalline domains and we checked that within our maximum simulation time, the system does not form crystallites in any of the 32 statistically independent simulation runs. The second model studied is a 50:50 binary mixture with a pairwise interactions that falls off with distance as an inverse power law,

$$V_{\alpha\beta}(r) = \epsilon_{\alpha\beta} \left( \frac{\sigma_{\alpha\beta}}{r} \right)^n, \quad (2)$$

with exponent  $n = 10$  (the **3dR10 model**). The potential is cut off at  $1.38\sigma_{\alpha\beta}$ . We again use a quadratic polynomial to make the potential and its first two derivative smooth at the cutoff. The parameters of the potential are:  $\epsilon_{\alpha\beta} = 1.0$ ,  $\sigma_{AA} = 1.0$ ,  $\sigma_{AB} = 1.22$  and  $\sigma_{BB} = 1.40$ . The temperature range covered for this model is  $T \in [0.52, 3.00]$  at number density  $\rho = 0.81$ . The same model with number density  $\rho = 0.85$  is studied in two dimensions. We will refer to this model as the **2dR10 model**. Length, energy and time scales are measured in units of  $\sigma_{AA}$ ,  $\epsilon_{AA}$  and  $\sqrt{\sigma_{AA}^2/\epsilon_{AA}}$ .

**Simulation Details:** NVT molecular dynamics simulations are performed in a cubic simulation box with periodic boundary conditions in both two and three dimensions for all the model systems. We use the modified leap-frog algorithm with the Berendsen thermostat to keep the temperature constant in the simulation runs. The use of any other thermostat does not change the results significantly as we are mostly interested in configurational changes in the system instead of momentum correlations. The integration time steps used is  $dt = 0.005$  in this temperature range. Equilibration runs are performed for  $\sim 10^8 - 10^9$  MD steps depending on the temperature and production runs are long enough to ensure that the two-point density correlation function  $Q(t)$  (defined below) goes to zero within the simulation time. For all the model systems, we have performed simulations for pin concentration (defined as the fraction of pinned particles) in the range  $\rho_{pin} \in [0.005, 0.200]$  for each temperature. For very low temperatures, we were not able to equilibrate the system for high pin concentrations because of a dramatic increase in the relaxation time.

**Dynamic Correlation Function:** Dynamics is characterized by the two point density-density overlap corre-

lation functions  $Q(t)$ , defined as:

$$Q(t) = \frac{1}{N - N_p} \left[ \left\langle \sum_{i,j=1}^{N-N_p} w(|\vec{r}_i(t) - \vec{r}_j(0)|) \right\rangle \right], \quad (3)$$

where the window function  $w(x) = 1.0$  if  $x < 0.30$ , else  $w(x) = 0$ . This choice of window function is made to remove the short-time vibrational component from the correlation function.  $N_p$  is the number of pinned particles in the system and  $\langle \dots \rangle$  implies thermal averaging and  $[\dots]$  means averaging over different realizations of the randomly pinned particles. We have calculated also the self part of the above correlation function, defined as

$$Q_s(t) = \frac{1}{N - N_p} \left[ \left\langle \sum_{i=1}^{N-N_p} w(|\vec{r}_i(t) - \vec{r}_i(0)|) \right\rangle \right]. \quad (4)$$

The relaxation time  $\tau_\alpha$  was obtained from  $Q_s(t)$  using  $Q_s(\tau_\alpha) = \exp(-1)$ .

**Pinning Protocol:** In this study, we have considered randomly pinned system in which the pinned particles are chosen randomly from an equilibrium configuration of the system at the temperature of interest. In [22] a different pinning protocol was used with the constraint that the pinning sites should be uniformly distributed in space. This, according to [22], reduces sample to sample fluctuations. However, in our study where we used random pinning without any bias, the sample to sample fluctuations are found to be similar in magnitude to those when the pinning protocol of Ref. [22] is used. So, we report here results obtained from simulations of randomly pinned systems in which the pinned particles were chosen without any bias. It is important to mention that different choices of the pinning protocol actually lead to somewhat different results, but whether the choice qualitatively changes the physics is yet to be understood.

**Configurational Entropy:** The configurational entropy is calculated here only for the unpinned systems and the per particle entropy is defined as

$$s_c = s_{bulk} - s_{vib} \quad (5)$$

where  $s_{bulk}$  is the bulk entropy calculated via thermodynamic integration and  $s_{vib}$  is the basin entropy for inherent structures, calculated using the harmonic approximation[27]. Similar analysis was recently extended to randomly pinned systems [22], although it is not clear whether the harmonic approximation is sufficiently accurate to get reliable estimates of the configurational entropy at the higher temperatures considered for the pinned systems [21].

**Static Length Scale:** The static length scale  $\xi_s$  is calculated from a combination of finite-size scaling of the minimum eigenvalue and point-to-set (PTS) methods as described in detail in Ref. [28] for the three dimensional

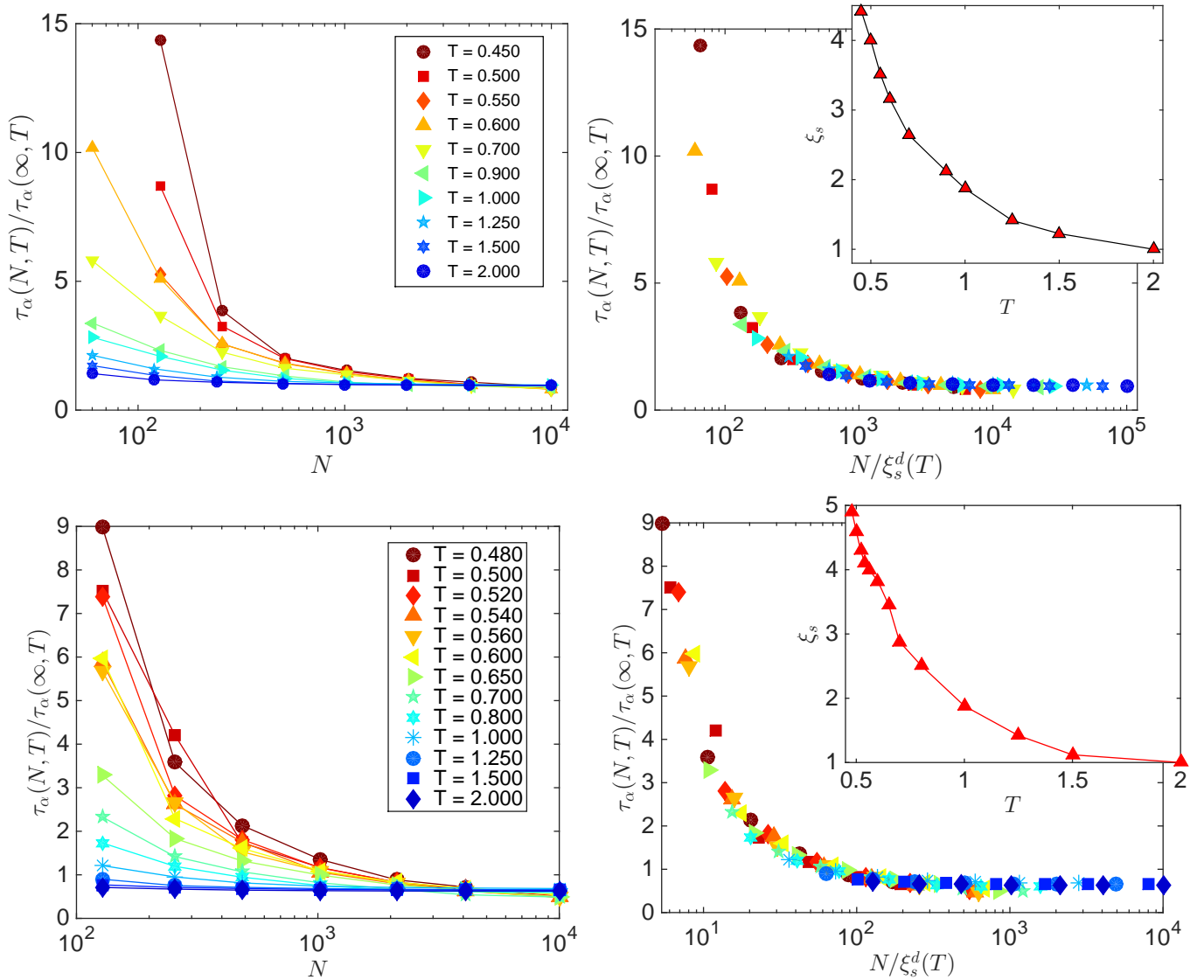


FIG. 1: Top Panels: Finite-size effects in the  $\alpha$  relaxation time of the 2dMKA model and the data collapse to obtain the static length scale  $\xi_s$  (shown in the inset). Bottom Panels: Similar analysis done for the 2dR10 model with the length scale shown in the inset (see text for details).

systems (3dKA and 3dR10). In Ref. [29], it was shown that the length scale obtained via the methods mentioned above for three dimensional systems completely explains the finite size effects seen in the relaxation time  $\tau_\alpha$  for all temperatures including high temperatures. So, for the two dimensional systems, we employed the method of finite-size scaling of  $\tau_\alpha$  to obtain the static length scales as the eigenvalue method and PTS methods involve much larger computational efforts to obtain the length scale. In Fig.1, we have shown the finite-size scaling of  $\tau_\alpha$  to obtain the static length scale for both the two dimensional models. The data collapses observed are quite good and that give us confidence about the reliability of the values of the extracted static length scale,

$\xi_s$ . There is a recent controversy about the usefulness of the PTS length scale for two-dimensional glass forming system with short-range bond-orientational order [31]. It is claimed that the PTS correlation length is insensitive to the growth of structural order in system with pronounced short-range bond-orientational order and hence the length scale associated with structural order, which governs the relaxation time, is not the same as the PTS length scale. It is to be noted that this controversy is not relevant for the two-dimensional systems considered here because local bond-orientational order is not pronounced in these systems.

### III. RANDOM FIRST ORDER TRANSITION THEORY

The Random First Order Transition (RFOT) [9–11] theory is motivated by analytic results obtained for infinite-range spin glass models whose behavior is qualitatively similar to that of structural glasses. This theory connects thermodynamics to dynamics via the configurational entropy  $s_c$ . The RFOT theory predicts certain relationships connecting the  $\alpha$ -relaxation time  $\tau_\alpha(T)$ , the static length scale  $\xi_s(T)$  and the configurational entropy  $s_c(T)$ , with associated exponents which have not yet been computed from any microscopic theory. The main ingredient of RFOT theory is the introduction of a surface free energy cost for creating an interface between two amorphous states of the same glassy system. Unlike conventional liquid-solid interfaces, the free energy cost of creating an interface between two amorphous states is somewhat difficult to define as there is no obvious order parameter which can distinguish between the two amorphous states. Direct measurements of this interfacial free energy cost have been attempted in the past, but a clear consensus on its dependence on the size of the interface is yet to emerge. Thus, a direct measurement of the interfacial free energy and the exponent that describes the power-law dependence of the free energy on the interface size would be very important for verifying the validity of the RFOT theory. In this work, we have tried to extract some of this information by introducing random pinning in the system and measuring the corresponding effects on the dynamics.

Close to the Kauzmann temperature  $T_K$ , RFOT theory predicts that the static correlation length  $\xi_s(T)$  diverges as

$$\xi_s(T) \propto \left[ \frac{1}{s_c(T)} \right]^{\frac{1}{d-\theta}}. \quad (6)$$

where the exponent  $\theta$  describes the dependence of the surface free energy cost on the linear size of the interface between two amorphous states. The  $\alpha$ -relaxation time is related to the static length-scale as

$$\tau_\alpha = \tau_0 \exp [\Delta \xi_s^\psi / T], \quad (7)$$

where it is assumed that the typical free energy barrier that has to be overcome in order to rearrange a correlated volume of linear size  $\xi_s$  is  $E_a = \Delta \xi_s^\psi$ . Substitution of Eq.6 in Eq.7 leads to a generalized Adam-Gibbs (AG) relation,

$$\tau_\alpha(T) = \tau_0 \exp \left[ \frac{A}{T s_c^{\frac{\psi}{d-\theta}}} \right] = \tau_0 \exp \left[ \frac{A}{T s_c^\alpha} \right], \quad (8)$$

where  $\alpha = \psi / (d - \theta)$ . The generalized AG relation, Eq. 8, reduces to the original AG relation if  $\psi = d - \theta$ . In this case, the Vogel-Fulcher-Tammann (VFT) form for the temperature dependence of  $\tau_\alpha$  is recovered if  $T s_c(T)$  goes to zero at the Kauzmann temperature  $T_K$

as  $T s_c(T) \propto (T - T_K)$ . Here we will work with the generalized AG relation, Eq. 8, as in [32], it was shown that the AG relation is violated in two dimensions and the nature of the deviation from the AG relation depends on the specific details of the model system studied. For a system that satisfies the generalized AG relation with  $\alpha \neq 1$ , the temperature dependence of  $\tau_\alpha$  would be described by the VFT equation if  $T s_c^\alpha \propto (T - T_K)$  for  $T$  close to  $T_K$ .

### IV. RANDOM PINNING: SCALING ARGUMENTS

In Ref. [18], it was argued that the Kauzmann temperature  $T_K$  where the configurational entropy  $s_c$  goes to zero should increase with increasing concentration  $\rho_{pin}$  of pinned particles. In Ref. [21],  $T_K$  was estimated by fitting the relaxation time  $\tau_\alpha$  as a function of temperature to the VFT formula for different values of  $\rho_{pin}$ . For many glass forming liquids without random pinning,  $T_K$  turns out to be close to the extrapolated VFT divergence temperature  $T_{VFT}$ . It was observed [21] that the  $T_{VFT}$  obtained from the fits does not increase with increasing pin concentration. Instead, the kinetic fragility decreases drastically as  $\rho_{pin}$  is increased. This behavior is in contradiction with the prediction in [18]. On the other hand, in Ref. [22],  $T_K$  was estimated by calculating the configurational entropy (using a harmonic approximation for the basin entropy) and it was found that  $T_K$  increases with increasing pin concentration. Based on this observation, the existence of an ideal glass state beyond a ‘‘critical’’ pin concentration was predicted. However, it has been shown explicitly in Refs. [21] and [23] that the self overlap function  $Q_s(t)$  and the self-intermediate scattering function decay to zero in time scales accessible in simulations even at state points where the configurational entropy is zero according to Ref [22]. This proves that the  $\alpha$  relaxation time remains finite [21] at the ideal glass state points obtained in Ref. [22]. This observation is in agreement with the finding in Ref. [21] that  $T_{VFT}$  does not increase with increasing  $\rho_{pin}$ .

A possible explanation of this discrepancy between the results for the dynamics and the configurational entropy was suggested in Ref. [24] where it was argued that one should extract the relaxation time from the total density correlation function instead of its self part. According to this argument, the total and self correlation functions decouple from each other as one increases the concentration of pinned particles and the relaxation time extracted from the total correlation function may diverge as  $s_c$  goes to zero, even if the time scale obtained from the self part remains finite. To test the validity of this argument, we have calculated the relaxation time from the total overlap correlation function for the 3dKA model at state points close the phase boundary in the  $(\rho_{pin} - T)$  plane obtained in Ref. [22]. In Fig.2, we have plotted the full overlap correlation function and its self part for two state points

near the phase boundary of Ref. [22] and extracted relaxation times from fits of the long-time data to a stretched exponential function. Since the full correlation function does not go to zero at long times (due to the presence of the random potential produced by the pinned particles), its long time value,  $Q(\infty)$ , was obtained from the fits and the quantity  $[Q(t) - Q(\infty)]/[1 - Q(\infty)]$ , which decays from one to zero as  $t$  is increased from zero to  $\infty$ , was used to obtain the relaxation time. The time scale obtained from the total overlap correlation function is found to be of the same order of magnitude, *but smaller than* that obtained from the self part. A similar conclusion was obtained from an analysis of the data for full and self correlation functions given in Ref. [24]. Thus, the discrepancy between the dynamics and the results for  $s_c(T)$  reported in [22] can not be resolved by considering the time scale obtained from the full density correlation function.

Here we will follow the arguments provided in Ref. [21] for understanding the dynamics of randomly pinned systems and use these arguments to analyze the simulation results obtained in the present study for both two and three dimensional glass forming liquids. In our analysis, we assume that: (a) the generalized AG relation of Eq.(8) remains valid for systems with pinning; and (b)  $Ts_c^\alpha(T)$  goes to zero at the Kauzmann temperature  $T_K$  as  $Ts_c^\alpha(T) \propto (T - T_K)$ , so that the temperature dependence of the  $\alpha$ -relaxation time follows the VFT form. The dependence of  $s_c$  on  $T$  and  $\rho_{pin}$  can be written as

$$\begin{aligned} Ts_c^\alpha(T, \rho_{pin}) &= Ts_c^\alpha(T, 0)F(T, \rho_{pin}) \\ &= K(T - T_K)F(T, \rho_{pin}), \end{aligned} \quad (9)$$

where  $F(T, \rho_{pin})$ , the fractional reduction of the configurational entropy due to pinning, decreases from 1 as  $\rho_{pin}$  is increased from 0. This is consistent with the general expectation of  $s_c$  being a decreasing function of  $\rho_{pin}$ . Our observation that the VFT temperature is independent of the value of  $\rho_{pin}$  implies, via the generalized Adam-Gibbs relation, that  $s_c$  goes to zero at the same temperature  $T_K$  for different values of  $\rho_{pin}$ . This, in turn, implies that for the small values of  $\rho_{pin}$  considered here,  $F(T, \rho_{pin})$  does not go to zero for temperatures higher than  $T_K$ . In Eq. 9,  $\alpha$  is the RFOT exponent defined in Eq. (8) and the second line follows from the expectation (verified in our simulations) that the temperature dependence of  $\tau_\alpha$  follows the VFT form. Eq.( 9) and the generalized Adam-Gibbs relation lead to the following expression for  $\tau_\alpha$  for non-zero  $\rho_{pin}$ :

$$\tau_\alpha(T, \rho_{pin}) = \tau_\infty \exp \left[ \frac{B(\rho_{pin})}{F(T, \rho_{pin})Ts_c^\alpha(T, 0)} \right]. \quad (10)$$

In Ref.[23], we have shown that  $\ln[\tau_\alpha(T, \rho_{pin})]$  varies linearly with  $1/[Ts_c^\alpha(T, 0)]$  for all the values of  $\rho_{pin}$  considered in our study. This behavior implies that  $F(T, \rho_{pin})$  is weakly dependent on or independent of  $T$ . We ignore the dependence of  $F$  on  $T$  in the following discussion. This equation predicts a VFT form for the temperature dependence of  $\tau_\alpha$ , with  $T_{VFT} = T_K$  independent of  $\rho_{pin}$ ,

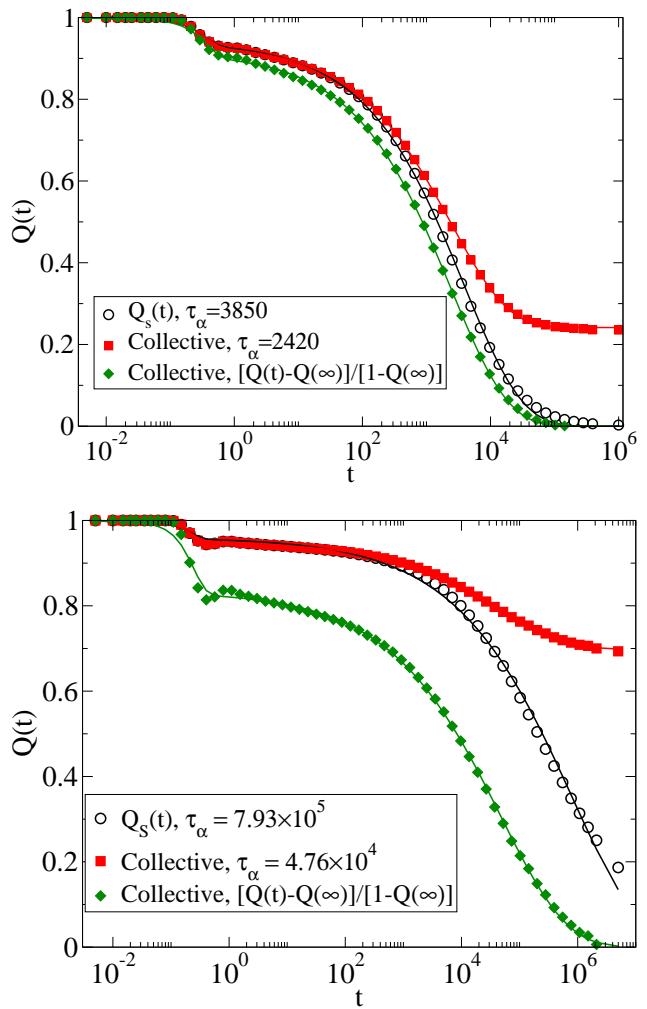


FIG. 2: Full overlap correlation function and its self part for the 3dKA model at two state points close to the phase boundary of Ref. [22]. *Top panel:* 3dKA,  $N = 1000$ ,  $T = 0.600$ ,  $\rho_{pin} = 0.120$ . *Bottom panel:* 3dKA,  $N = 300$ ,  $T = 0.700$ ,  $\rho_{pin} = 0.300$ . Solid lines represent fits to the data points (see text for details). The time scale of decay of the full correlation function is shorter than that for the self part.

in agreement with the observations in Ref. [21]. The fragility parameter  $K_{VFT} = KT_{VFT}F(\rho_{pin})/B(\rho_{pin})$  would decrease with increasing  $\rho_{pin}$  (i.e. would agree with our observations) if  $F/B$  is a decreasing function of  $\rho_{pin}$ . This condition would be satisfied if  $B$  increases, remains constant or decreases slower than  $F$  with increasing  $\rho_{pin}$ .

From Eq.(10), we get

$$\ln \left[ \frac{\tau_\alpha(T, \rho_{pin})}{\tau_\alpha(T, 0)} \right] = G(\rho_{pin})/[Ts_c^\alpha(T, 0)] \quad (11)$$

where

$$G(\rho_{pin}) \equiv \frac{B(\rho_{pin})}{F(\rho_{pin})} - \frac{B(0)}{F(0)}. \quad (12)$$

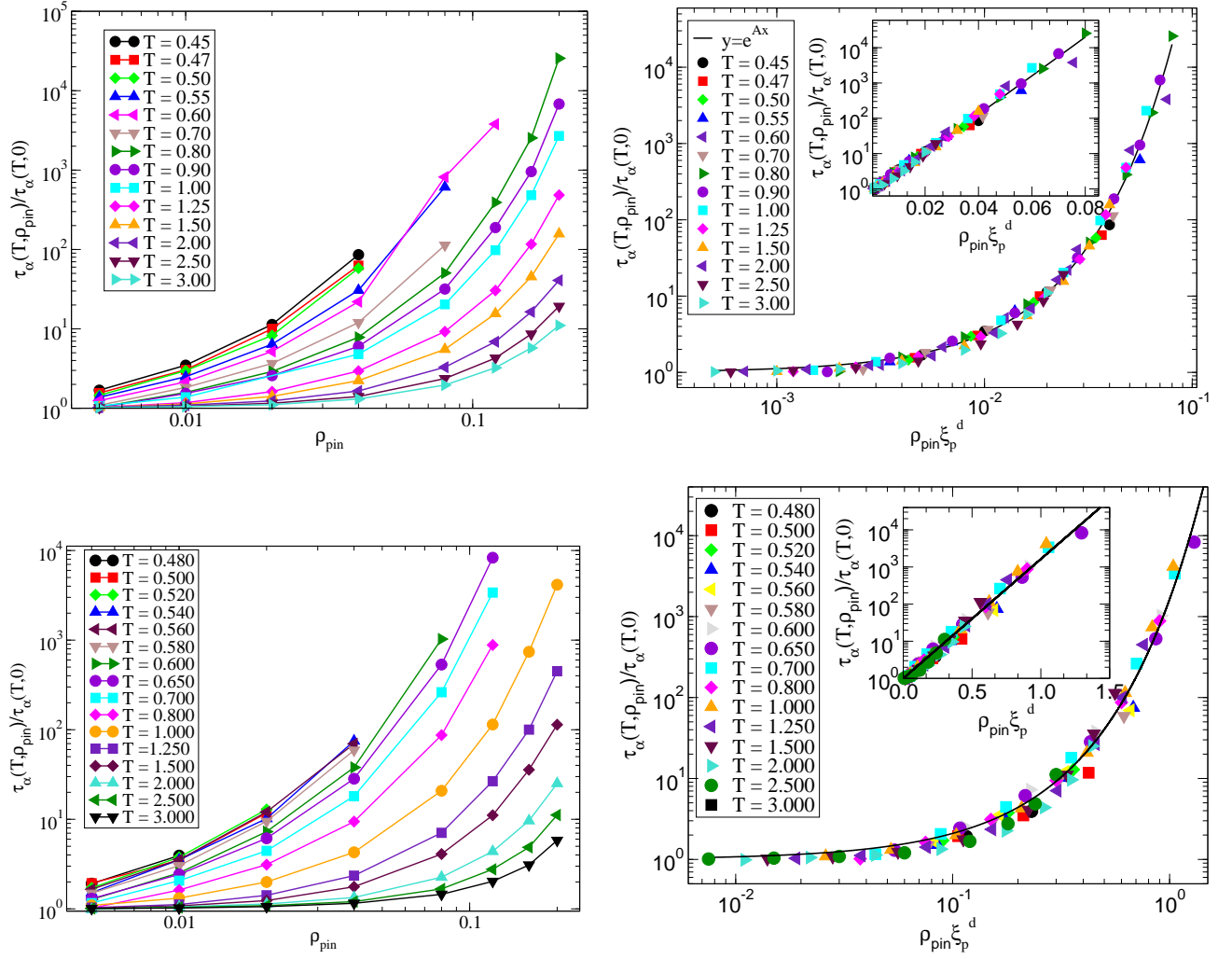


FIG. 3: Data collapse using the form in Eq. 14 to obtain the length-scale  $\xi_p$ . The upper panels are for the 2dMKA system and the lower panels are for the 2dR10 system. The left panels show the uncollapsed data. The lines passing through the collapsed data in both upper and lower right panels represent the scaling function in Eq.14. The scaling function provides a good description of the collapsed data in both cases. Insets in both upper and lower panels represent the collapsed data in log-linear scale. The nice straight line passing through the data clearly confirms our scaling arguments.

Clearly,  $G(0)$  is equal to zero and for small values of  $\rho_{pin}$ , we can write  $G(\rho_{pin}) = C\rho_{pin} + C'\rho_{pin}^2 + \dots$ , where  $C$  and  $C'$  are constants and  $\dots$  represent term with higher powers of  $\rho_{pin}$ . Using this in Eq.(11) above, we get

$$\ln \left[ \frac{\tau_\alpha(T, \rho_{pin})}{\tau_\alpha(T, 0)} \right] = (C\rho_{pin} + C'\rho_{pin}^2 + \dots) / [Ts_c^\alpha(T, 0)]. \quad (13)$$

For small values of  $\rho_{pin}$ , we can retain only the term linear in  $\rho_{pin}$  in the right-hand side of Eq.(13) and obtain the following scaling relation:

$$\ln \left[ \frac{\tau_\alpha(T, \rho_{pin})}{\tau_\alpha(T, 0)} \right] = Cf(\rho_{pin}\xi_p^d(T)) \quad (14)$$

with  $f(x) = x$  and the pinning length scale  $\xi_p$  is given by

$$\xi_p(T) = [1/(Ts_c^\alpha(T, 0))]^{1/d} \propto [1/(T - T_{VFT})]^{1/d} \quad (15)$$

where  $d$  is the spatial dimension. It is clear from its derivation that the scaling relation of Eq.(14) is valid only for small values of  $\rho_{pin}$ . As shown below, this scaling relation is satisfied by our numerical data in both two and three dimensions, indicating that for a fixed temperature  $T$ , the quantity  $\ln[\tau_\alpha(T, \rho_{pin})/\tau_\alpha(T, 0)]$  is proportional to  $\rho_{pin}$  for the small values of  $\rho_{pin}$  considered in our work (see the insets of the right panels of Fig. 3).

The length scale  $\xi_p$  can be identified as the average separation between neighboring pinned particles required for producing a given pinning-induced fractional change in the relaxation time. Let us consider a small pinning-induced fractional change in the relaxation time, i.e.  $\tau_\alpha(T, \rho_{pin})/\tau_\alpha(T, 0) = 1 + x$  where the fractional change  $x$  is a small positive number. Putting this in Eq.(14), we

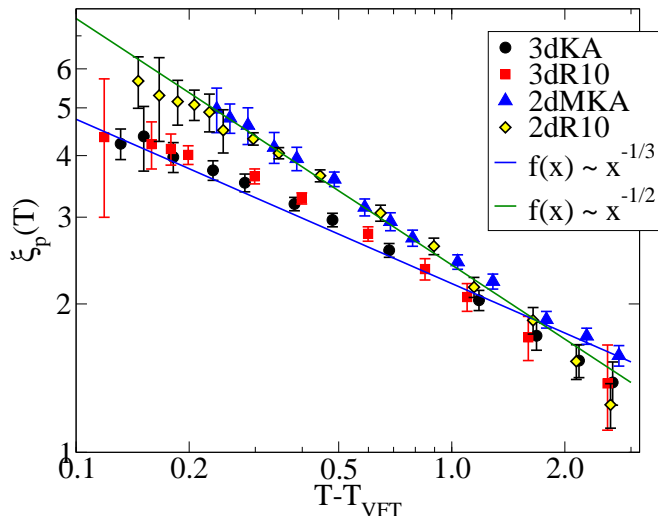


FIG. 4:  $\xi_p$  vs  $(T - T_{VFT})$  to demonstrate the validity of the scaling predictions.

get

$$\ln(1+x) \simeq x = C\rho_{pin}\xi_p^d(T), \quad (16)$$

which can be written as

$$\left(\frac{1}{\rho_p}\right)^{1/d} = \left(\frac{C}{x}\right)^{1/d} \xi_p(T). \quad (17)$$

Since  $(1/\rho_{pin})^{1/d}$  is proportional to the average distance between neighboring pinned particles,  $\xi_p(T)$  is proportional to the average pin separation required for producing a given fractional change  $x$  in the relaxation time at temperature  $T$ . The increase of the length scale  $\xi_p(T)$  with decreasing  $T$  means that at lower temperatures, a larger pin separation (smaller pin concentration) would be required for producing the same fractional change in the relaxation time. A very similar length scale with  $\alpha = 1$  was introduced in Ref.[18], in which it was interpreted as “the critical mean distance between frozen particles”. We are not aware of any correlation function whose spatial decay is governed by the length scale  $\xi_p$ .

This scaling prediction was tested and verified in Ref. [21] for both the three dimensional models considered here. As shown in Fig. 3, it is possible to collapse all the data for  $\psi(T, \rho_{pin}) \equiv \ln[\tau_\alpha(T, \rho_{pin})/\tau_\alpha(T, 0)]$  for each of the two dimensional models into a single scaling curve by choosing the length scale  $\xi_p(T)$  appropriately for different temperatures. The scaling function, represented by the line passing through the collapsed data points, is indeed of the form predicted by the scaling argument.

To check whether the  $\xi_p(T)$  obtained from the scaling collapse is proportional to  $[1/(T - T_{VFT})]^{1/d}$ , we have plotted in Fig. 4 the pinning length scale  $\xi_p$  obtained from the scaling collapse in Fig. 3 as a function of  $(T - T_{VFT})$  for all the model systems. The results

are clearly consistent with the predicted behavior. Thus, the scaling description proposed in Ref. [21] provides a consistent description of the simulation data in both two and three dimensions. A very similar scaling description has been used [34] in a recent study to understand experimental results for the dynamics of a confined colloidal system.

## V. RFOT EXPONENTS $\theta$ AND $\psi$

In this section, we use the results for  $\xi_p(T)$ ,  $\xi_s(T, 0)$ ,  $s_c(T, 0)$  and  $\tau_\alpha(T, 0)$  to estimate the values of the RFOT exponents  $\theta$  and  $\psi$  for the unpinned system. The exponent  $\psi$  is obtained from the data for  $\xi_p$  and  $\xi_s$  (see Fig.5). The exponent  $\alpha = \psi/(d - \theta)$  for the two-dimensional models ( $\alpha = 1$  for the three-dimensional models) is obtained from the generalized AG relation (see Fig. 7 - Fig. 8 shows that the values of  $\alpha$  obtained from the fits in Fig. 8 are consistent with the VFT form for the temperature dependence of  $\tau_\alpha(T, 0)$ ). The value of  $\theta$  is obtained from the calculated values of  $\psi$  and  $\alpha$ . Finally, Fig. 6 provides a consistent check by examining whether the RFOT relation of Eq.(6) is satisfied for the calculated values of the exponent  $\theta$ .

The range of our data for the correlation lengths  $\xi_s$  and  $\xi_p$  is less than one decade. This is not sufficient for an accurate determination of the power-law exponents. This difficulty in obtaining data over a range that is large enough to determine the RFOT exponents with high accuracy is intrinsic to the glass transition problem. Since the liquid falls out of equilibrium at temperatures substantially higher than the putative RFOT transition at  $T_K$ , the relevant correlation lengths  $\xi_s$  and  $\xi_p$  remain relatively small in the temperature range accessible in experiments or simulations. For this reason, all existing attempts to determine the RFOT exponents from simulations [35, 36] and experiments [37] are based on data that span ranges comparable to or smaller than the ranges considered in our work. The novelty of our work is that we have used results for the dynamics in the presence of pinning to estimate the values of these exponents.

It follows from Eq. 6 and Eq. 15 that

$$T\xi_p^d(T) = \frac{1}{s_c^\alpha(T, 0)} \propto \xi_s^\psi(T, 0). \quad (18)$$

Thus, the data for  $\xi_p(T)$  and  $\xi_s(T, 0)$  can be used to estimate the RFOT exponent  $\psi$ . In Fig.5,  $\ln(T\xi_p^d)$  is plotted *versus*  $\ln(\xi_s)$  for all the four models considered here. The exponent  $\psi$  obtained from the slope of this plot turns out to be close to unity for the two models studied in three dimensions. The best fit values, indicated by straight lines in the figure, are  $\psi = 0.967$  for the 3dKA model and  $\psi = 1.07$  for the 3dR10 model. The observation [32] that the AG relation is obeyed in both three dimensional models implies that  $\alpha = \psi/(d - \theta) = 1$  in three dimensions. This result, in combination of the result for  $\psi$ , imply that  $\theta \simeq 2.0$  in three dimensions. Our data for



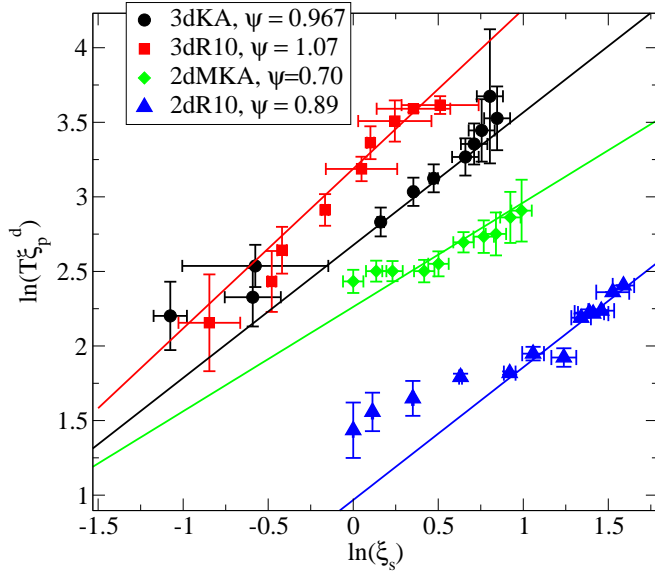


FIG. 5:  $T\xi_p^d$  vs  $\xi_s$  to extract the exponent  $\psi$ . Only the low temperature data points are fitted.

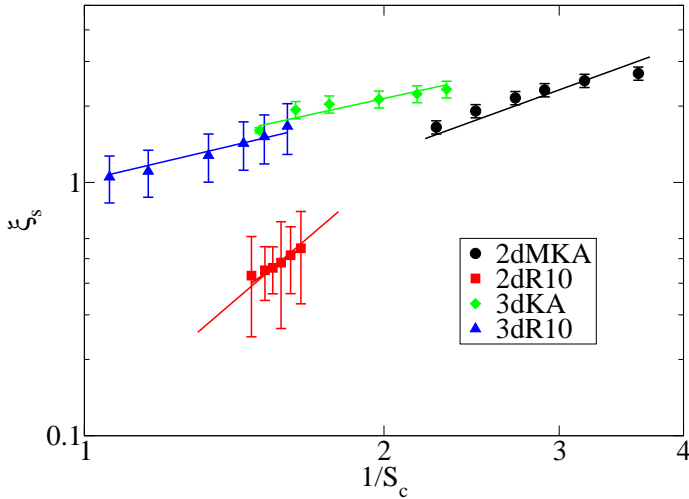


FIG. 6: The static length scale  $\xi_s$  is plotted as a function of  $1/s_c$  for all the four model systems. The solid lines are fits to the form  $\xi_s \propto (1/s_c)^{1/(d-\theta)}$  with  $d-\theta$  obtained from the relation  $\psi = \alpha(d-\theta)$ . The values of  $\psi$  are obtained from the fits shown in Fig. 5,  $\alpha = 1$  for the three dimensional models and  $\alpha$  for the two dimensional models are obtained from the fits shown in Fig. 7.

the dependence of  $\xi_s$  on  $s_c$  are also consistent with Eq.6. In Fig.6,  $\xi_s$  is plotted as a function of  $1/s_c$  for both the model systems and Eq.6 with  $(d-\theta)$  obtained from the relation  $\psi = \alpha(d-\theta)$  provides a good description of the data for the three dimensional model systems.

For the two dimensional models, the AG relation is violated [32] and the relation  $\alpha = \psi/(d-\theta) = 1$  is not

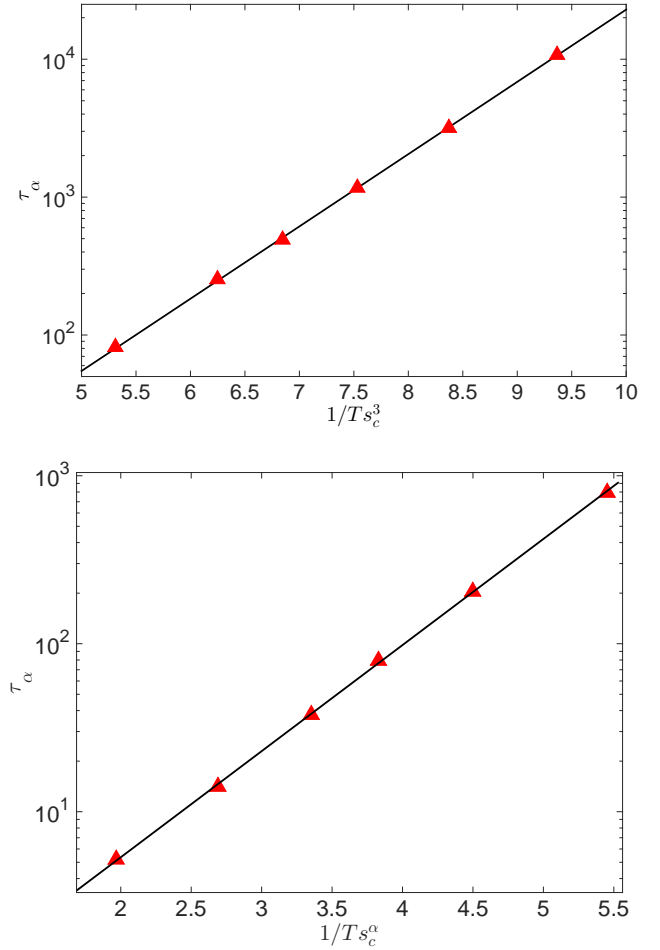


FIG. 7: Top Panel: Modified Adam-Gibbs relation for the 2dR10 model. Bottom Panel: Similar plot for the 2dMKA model with  $\alpha \simeq 0.70$ .

satisfied. We have obtained the exponent  $\psi$  from Eq.18 and  $\psi/(d-\theta)$  from the modified AG relation for the unpinned system. For the 2dMKA model,  $\psi \simeq 0.70$  (see Fig. 5), when only the low temperature data are considered and  $\psi/(d-\theta) \simeq 0.70$  from the generalized AG plot shown in Fig. 7. Thus,  $\theta \simeq 1.0$  for this model. In the  $\xi_s$  vs  $1/s_c$  plot in Fig. 6,  $\theta \simeq 1.0$  describes the data quite well. Also, the relation  $s_c^\alpha(T) \propto (T - T_K)$ , required for the validity of the VFT form, is satisfied for  $\alpha = 0.70$ , as shown in Fig. 8.

For the 2dR10 model,  $\psi \simeq 0.89$  from Fig. 5 if only the low temperature data are considered. A smaller value of  $\psi$  ( $\sim 0.75$ ) is obtained if the data for a wider range of temperature are used in the power-law fit. The modified AG relation gives  $\alpha = \psi/(d-\theta) \simeq 3.0$  (see Fig. 7). This implies  $\theta \simeq 1.70$ . The data for  $\xi_s$  and  $1/s_c$  are consistent with the expected relation between these two quantities with  $d-\theta \simeq 0.29$  (see Fig.6). Also, as shown in Fig. 8, the relation  $s_c^\alpha(T) \propto (T - T_K)$  is satisfied by the data with  $\alpha = 3.0$ . However, the value of  $\theta$  violates the phys-

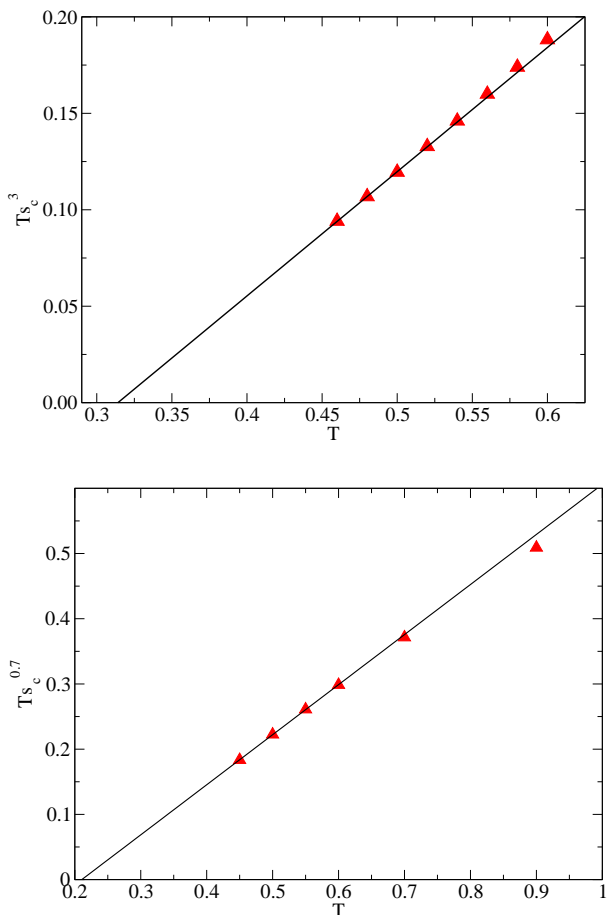


FIG. 8: Top Panel:  $Ts_c^\alpha$  vs  $T$  plot for the 2dR10 model with  $\alpha = 3.0$ . Bottom Panel: Similar plot for the 2dMKA model with  $\alpha = 0.70$ . Fairly good straight line fits at lower temperatures suggest that the relation  $Ts_c^\alpha \propto T - T_K$  is satisfied, indicating that the VFT law will be obeyed.

ically expected condition,  $\theta \leq d - 1$ . Thus, although the exponent values  $\psi \simeq 0.89$ ,  $\alpha \simeq 3.0$ ,  $\theta \simeq 1.70$  provide an internally consistent description of the simulation data, the value of  $\theta$  turns out to be unphysical. This unphysical value of  $\theta$  is a consequence of the rather large value of  $\alpha$ . For  $\theta$  to be less than  $(d - 1)$  in two dimensions, the exponents  $\psi$  and  $\alpha$  must satisfy the inequality  $\alpha < \psi$ . This is clearly ruled out by the data. The value of  $\alpha$  reported in Ref. [32] for the 2dR10 model ( $\alpha \simeq 2.1$ ) would also lead to a value of  $\theta$  ( $\simeq 1.5$ ) that is higher than  $(d - 1)$ .

Our results for the three-dimensional models ( $\psi \simeq 1$  and  $\theta \simeq 2$ ) are consistent with those reported in Refs. [35] and [36]. These values are different from those reported in Ref. [8] for the 3dKA model because the length scale considered in that work was the dynamic length scale which is distinct from the static length scale  $\xi_s$  considered here. The results for the two-dimensional models indicate that the exponent values are not universal. It is also possible that the RFOT description breaks down in two

dimensions.

## VI. FRAGILITY AND THE STATIC LENGTH SCALE

As discussed in the Introduction, kinetic fragility measures the rate at which the relaxation time changes with decreasing temperature. The role of fragility can be clearly demonstrated by plotting the relaxation time scaled by its infinite temperature value as a function of the temperature scaled by  $E_\infty$ , the high temperature activation energy scale obtained by fitting the high temperature relaxation time data to the Arrhenius form,

$$\frac{\tau_\alpha(T)}{\tau_\infty} = \exp\left(\frac{E_\infty}{T}\right). \quad (19)$$

This way of plotting the relaxation time data for different systems makes sure that the high temperature part of the data for all the systems fall on a single master curve which would be a straight line if  $\ln(\tau_\alpha/\tau_\infty)$  is plotted as a function of  $E_\infty/T$ . Deviations from this straight line at lower temperatures would highlight the varying degree of fragility of these different systems. In the left panels of Fig. 9 and Fig. 10, one can clearly see that the relaxation time data at high temperatures fall on a straight line. Values of the parameters  $E_\infty$  and  $\tau_\infty$ , obtained from fits of the high-temperature data to the Arrhenius form of Eq. 19 are given in Table I for all the models considered here. The data for systems with different values of  $\rho_{pin}$  deviate from this straight line by different amounts at low temperatures. The unpinning system deviates the most and the system with  $\rho_{pin} = 0.20$  shows the least amount of deviation, illustrating a decrease of fragility with increasing pin density.

	3dKA		3dR10		2dMKA		2dR10	
$\rho_{pin}$	$E_\infty$	$\tau_\infty$	$E_\infty$	$\tau_\infty$	$E_\infty$	$\tau_\infty$	$E_\infty$	$\tau_\infty$
0.000	2.648	0.133	2.765	0.093	2.773	0.280	2.741	0.213
0.005	2.698	0.130	2.731	0.095	2.794	0.284	2.793	0.209
0.010	2.828	0.124	2.800	0.093	3.015	0.271	2.926	0.204
0.020	2.986	0.120	2.962	0.088	3.583	0.234	3.345	0.181
0.040	3.210	0.115	3.073	0.087	4.528	0.198	4.277	0.140
0.080	3.823	0.103	3.717	0.072	6.078	0.178	6.164	0.092
0.120	-	-	4.224	0.064	7.600	0.177	8.233	0.065
0.160	5.201	0.084	5.228	0.048	9.180	0.187	10.233	0.052
0.200	6.270	0.070	5.615	0.047	10.834	0.210	11.939	0.057

TABLE I: Values of  $E_\infty$  and  $\tau_\infty$  for different pin concentrations, obtained from the fits shown in Figs. 9 and 10.

If the relaxation time  $\tau_\alpha$  is determined solely by the static length scale  $\xi_s$ , as in Eq. 7 with  $\Delta$  a system dependent constant, then one would expect that the fragility will also be completely determined by the growth of the static length scale with decreasing temperature. If the exponent  $\psi$  is the same for systems with different pin

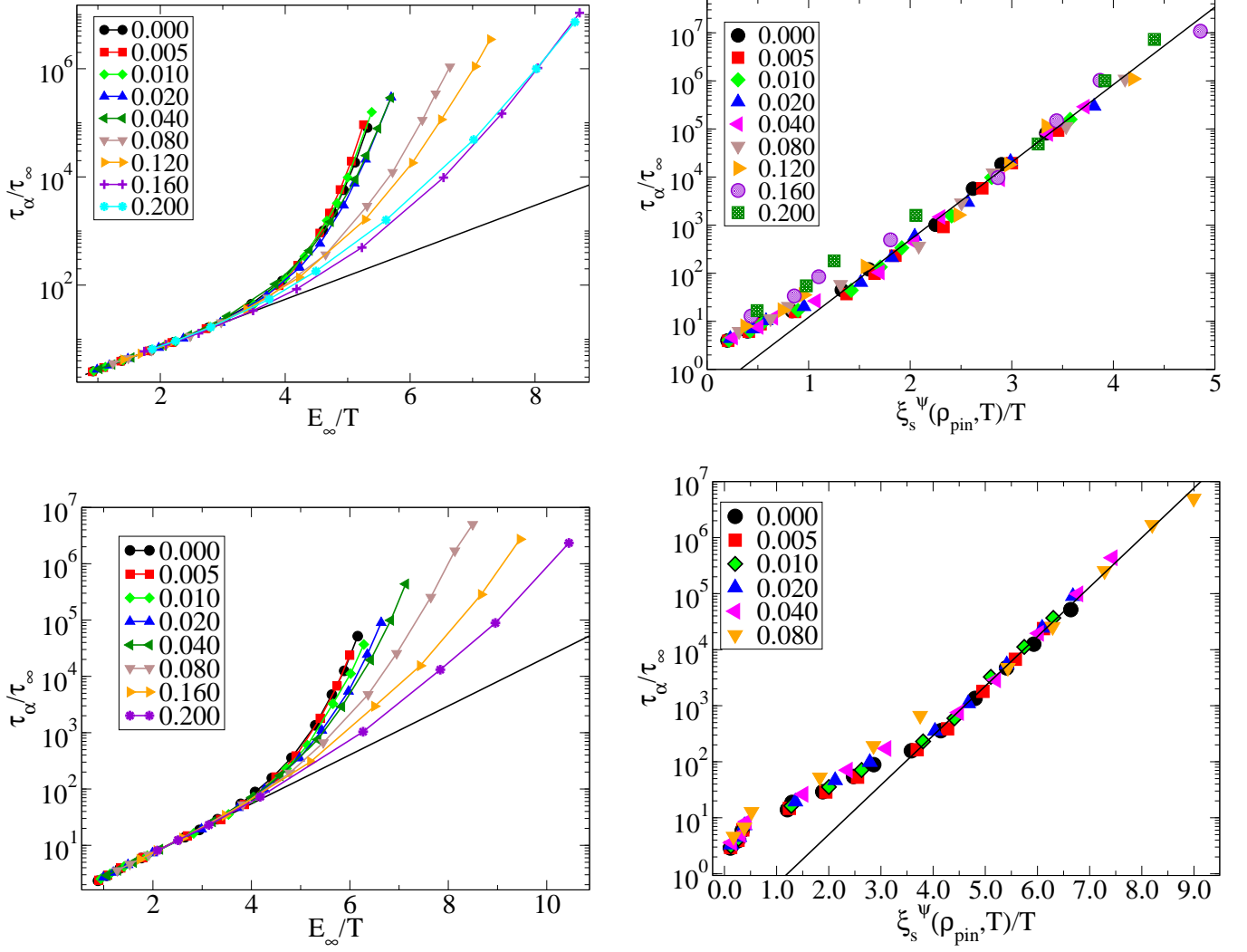


FIG. 9: *Top Left panel:*  $\tau_\alpha/\tau_\infty$  versus  $E_\infty/T$  for the 3dKA model with varying levels of pinning. *Top Right panel:* Data collapse using the static length scale  $\xi_s(T, \rho_{pin})$ . The data collapse is not good for higher levels of pinning since the scaling arguments presented in the text are valid in the weak pinning regime. *Bottom panels:* Similar analysis for the 3dR10 model. The values of  $E_\infty$  and  $\tau_\infty$  are provided in Table I. For the 3dKA model,  $\psi = 0.967$  and for the 3dR10 model,  $\psi = 1.07$ .

densities, then plots of the scaled relaxation time as a function of  $\xi_s^\psi(T, \rho_{pin})/T$  should collapse to a straight line at low temperatures. This possibility is checked below by approximately calculating the static length scale for different pin densities. The objective here is to examine whether the observed fragility change with increasing pin concentration can be understood as an effect of a pinning-induced change in the temperature dependence of the static length scale.

We start from our proposal for the dependence of the configurational entropy on pin concentration, Eq.9. For small pin concentrations,  $\rho_{pin} \rightarrow 0$ , we can express  $F(\rho_{pin})$  as  $F(\rho_{pin}) = 1 - C\rho_{pin} + \dots$ ,  $C > 0$  and the corresponding configurational entropy as

$$s_c(T, \rho_{pin}) = s_c(T, 0)(1 - C\rho_{pin}). \quad (20)$$

Now, assuming that the RFOT relation between the

static length scale and the configurational entropy (Eq. 6) remains valid for pinned systems, we can write

$$\begin{aligned} \xi_s(T, \rho_{pin}) &\propto \left[ \frac{1}{T s_c(T, \rho_{pin})} \right]^{1/(d-\theta)} \\ &= D(\rho_{pin}) \left[ \frac{1}{T s_c(T, 0)} \right]^{\frac{1}{d-\theta}} \end{aligned} \quad (21)$$

with  $D(\rho_{pin}) = 1 + A\rho_{pin} + \dots$ ,  $A > 0$ . Thus, we have

$$\xi_s(T, \rho_{pin}) = \xi_s(T, 0)(1 + A\rho_{pin}). \quad (22)$$

As discussed earlier, the static length scale for  $\rho_{pin} = 0$  for the three dimensional models is obtained from a combination of finite size scaling analysis of the minimum eigenvalue of the Hessian matrix and PTS analysis (see [28] for further details). Finite size scaling of  $\tau_\alpha$  is used

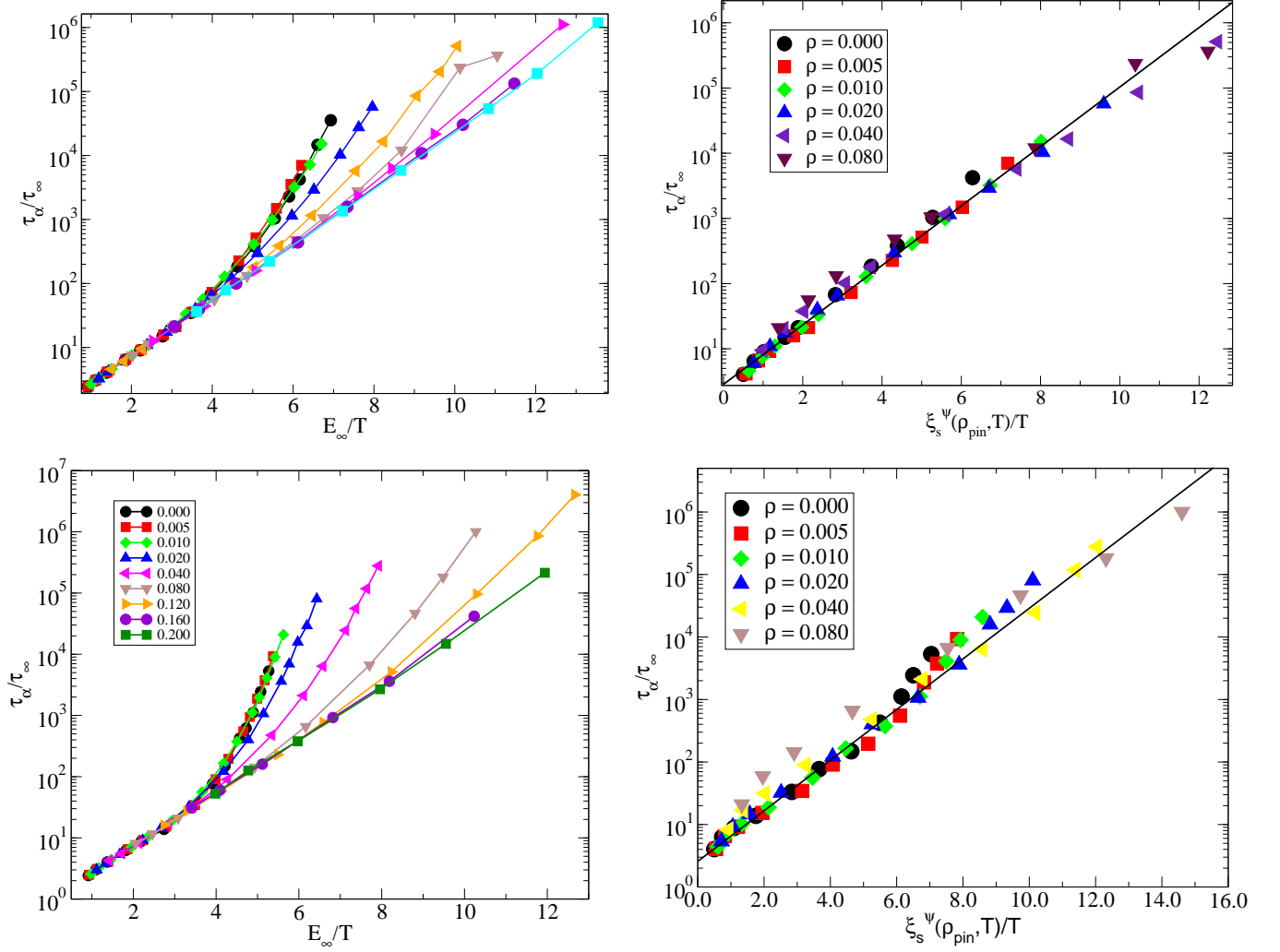


FIG. 10: *Top Left panel:*  $\tau_\alpha/\tau_\infty$  versus  $E_\infty/T$  for the 2dMKA model with varying levels of pinning. *Top Right panel:* Data collapse using the static length scale  $\xi_s(T, \rho_{pin})$ . The data collapse is not good for higher levels of pinning since the scaling arguments presented in the text are valid in the weak pinning regime. *Bottom panels:* Similar analysis for the 2dR10 model. The values of  $E_\infty$  and  $\tau_\infty$  are provided in Table I. For the 2dMKA model,  $\psi = 0.70$  and for the 2dR10 model,  $\psi = 0.89$ .

to extract the static length scale for the two dimensional model systems studied here. Once the length scale at zero pinning is obtained, Eq.22 is used to obtain the static length scale for different pin densities, treating  $A$  as a system dependent constant. This length scale is then used to obtain the data collapse in Figs. 9 and 10. The value of  $A$  for each model system is determined by maximizing the quality of data collapse. The collapse of the  $\tau_\alpha$  data for varying levels of pinning is observed to be quite good within our numerical accuracy. The data for the larger values of  $\rho_{pin}$ ,  $\rho_{pin} \in \{16\%, 20\%\}$  could not be collapsed for the 3dKA model, suggesting that in this case, one may need to include higher order terms in Eq.22. This analysis suggests a deep connection between the static length scale and the fragility in different glass forming liquids.

## VII. CONCLUSIONS

In this article we have presented results from extensive computer simulations of the dynamics of several model glass forming liquids in the presence of random pinning in both two and three dimensions. The effects of random pinning on the dynamics of two dimensional systems are found to be qualitatively similar to those reported earlier [21] for three dimensional model glass formers. The presence of random pinning does not lead to an increase in the VFT temperature  $T_{VFT}$ , but increases the kinetic fragility of the liquids, irrespective of the model and the spatial dimension considered in the simulation. We have tried to understand the observed behavior within the framework of the RFOT theory and provided a scaling description that explains our simulation results for the dependence of the  $\alpha$  relaxation time and the fragility on

the pin concentration.

The main results of this work are:

- The fragility of a glass forming liquid can be tuned systematically over a large range by pinning a randomly chosen subset of the particles in their equilibrium positions. This effect is generic for glass forming liquids in both two and three dimensions.
- We find that pinning induced changes in the temperature dependence of the  $\alpha$  relaxation time  $\tau_\alpha$  can be explained entirely in terms of the dependence of the static length scale of RFOT,  $\xi_s(T, \rho_{pin})$ , on the pin concentration  $\rho_{pin}$ . This observation implies that the kinetic fragility is intimately connected with the static length scale. In particular, the RFOT relationship between  $\tau_\alpha$  and  $\xi_s$ ,  $\tau_\alpha = \tau_0 \exp(\Delta\xi_s^\psi/T)$  describes the data quite well and appears to be universal in nature.
- A scaling description, consistent with the RFOT theory and based on the assumption that random pinning changes the configurational entropy by a multiplicative factor that decreases from unity as the pin concentration is increased from zero, provides a good description of all simulation results for the dynamics. This description reveals the existence of a pinning-related static length scale,  $\xi_p$ . The dynamics of supercooled liquids with random pinning can be completely understood in terms of this length scale and the other static length scale,  $\xi_s$ . A scaling argument suggests the existence of a simple relation between these two length scales and gives us an opportunity to extract one of the exponents (the barrier height exponent  $\psi$ ) of RFOT theory from the simulation data.
- Combining the results for  $\psi$  with those for the exponent  $\alpha$  in the generalized AG relation, we can extract the value of the RFOT surface tension exponent  $\theta$ . Our results for the three dimensional models are consistent with  $\theta = (d - 1)$ ,  $\psi = 1$ . In one of the two dimensional models (the 2dMKA model), we find  $\theta \simeq d - 1$ ,  $\psi \simeq 0.7$ . In the other two dimensional model (the 2dR10 model), the value of  $\psi$  is found to be close to 1, but the value of  $\theta > 1.0$  violates the inequality  $\theta \leq (d - 1)$ . This suggests that the RFOT description is not applicable to this system. Our results for the two dimensional systems are consistent with earlier observation [32] of breakdown of the AG relation and lack of universality in two dimensions. This may be related to recent results [33] suggesting that the behavior of glass forming liquids in two dimensions is qualitatively different from that observed in three dimensions.
- Relations among the static length scale  $\xi_s$ , the configurational entropy  $s_c$  and the  $\alpha$  relaxation time  $\tau_\alpha$  predicted in the RFOT theory are satisfied by our simulation results with the obtained exponent values.

In conclusion, this study clearly demonstrate that many of the simulation results for the dynamics of different glass forming liquids in the presence of random pinning can be understood within the framework of the RFOT theory and random pinning provides an interesting tool to unravel several aspects of glassy dynamics. More simulational and experimental research along these lines will be very useful.

- 
- [1] A. Cavagna, Phys. Rep. **476**, 51 (2009).
- [2] L. Berthier and G. Biroli, Rev. Mod. Phys. **83**, 587 (2011).
- [3] S. Karmakar, C. Dasgupta, and S. Sastry, Annu. Rev. Condens. Matter Phys. **5**, 255 (2014).
- [4] M. D. Ediger, Annu. Rev. Phys. Chem. **51**, 99 (2000).
- [5] L. Berthier, G. Biroli, J.-P. Bouchaud, L. Cipelletti, D. E. Masri, D. L'Hte, F. Ladieu, and M. Pierno, Science **310**, 1797 (2005).
- [6] G. Biroli, J.-P. Bouchaud, K. Miyazaki, and D. R. Reichman, Phys. Rev. Lett. **97**, 195701 (2006).
- [7] G. Biroli, J.-P. Bouchaud, A. Cavagna, T. S. Grigera, and P. Verrocchio, Nat. Phys. **4**, 771 (2008).
- [8] S. Karmakar, C. Dasgupta, and S. Sastry, Proc. Nat'l Acad. Sci. USA **106**, 3675 (2009).
- [9] T. R. Kirkpatrick, D. Thirumalai, and P. G. Wolynes, Phys. Rev. A **40**, 1045 (1989).
- [10] V. Lubchenko and P. G. Wolynes, Annu. Rev. Phys. Chem. **58**, 235 (2007).
- [11] G. Biroli and J.-P. Bouchaud, Structural Glasses and Supercooled Liquids: Theory, Experiment, and Applications pp. 31–113 (2012).
- [12] C. A. Angell, in *Relaxation in complex systems*, edited by K. L. Ngai and G. B. Wright (Naval Research Laboratory, Washington DC, 1985), pp. 3–11.
- [13] S. E. Abraham, S. M. Bhattacharrya, and B. Bagchi, Phys. Rev. Lett. **100**, 167801 (2008).
- [14] D. Coslovich and G. Pastore, J. Chem. Phys. **127**, 124504 (2007).
- [15] L. Berthier and T. A. Witten, Europhys. Lett. **86**, 10001 (2009).
- [16] S. Sengupta, F. Vasconcelos, F. Affouard, and S. Sastry, J. Chem. Phys. **135**, 194503 (2011).
- [17] A. D. S. Parmar and S. Sastry, J. Phys. Chem. B (2015).
- [18] C. Cammarota and G. Biroli, Proc. Nat'l Acad. Sci. USA **109**, 8850 (2012).
- [19] W. Kob and L. Berthier, Phys. Rev. Lett. **110**, 245702 (2013).
- [20] W. Kob and D. Coslovich, Phys. Rev. E **90**, 052305 (2014).
- [21] S. Chakrabarty, S. Karmakar, and C. Dasgupta, Sci. Rep. **5**, 12577 (2015).

- [22] M. Ozawa, W. Kob, A. Ikeda, and K. Miyazaki, Proc. Nat'l Acad. Sci. USA p. 201500730 (2015).
- [23] S. Chakrabarty, S. Karmakar, and C. Dasgupta, Proc. Nat'l Acad. Sci. USA **112**, E4819 (2015).
- [24] M. Ozawa, W. Kob, A. Ikeda, and K. Miyazaki, Proc. Nat'l Acad. Sci. USA **112**, E4821 (2015).
- [25] S. Gokhale, K. H. Nagamanasa, R. Ganapathy, and A. Sood, Nat. Commun. **5** (2014).
- [26] W. Kob and H. C. Andersen, Phys. Rev. E **51**, 4626 (1995).
- [27] S. Sastry, Phys. Rev. Lett. **85**, 590 (2000).
- [28] G. Biroli, S. Karmakar, and I. Procaccia, Phys. Rev. Lett. **111**, 165701 (2013).
- [29] S. Karmakar, C. Dasgupta, and S. Sastry, Rep. Prog. Phys. **79**, 016601 (2016).
- [30] S. Karmakar and I. Procaccia, Phys. Rev. E **86**, 061502 (2012).
- [31] J. Russo and H. Tanaka, Proc. Nat'l Acad. Sci. USA **112**, 6920 (2015).
- [32] S. Sengupta, S. Karmakar, C. Dasgupta, and S. Sastry, Phys. Rev. Lett. **109**, 095705 (2012).
- [33] E. Flenner and G. Szamel, Nat. Commun. **6** (2015).
- [34] B. Zhang and X. Cheng, Phys. Rev. Lett. **116**, 098302 (2016).
- [35] C. Cammarota, A. Cavagna, G. Gradenigo, T. S. Grigera, and P. Verrochio, J. Phys. Chem **131**, 194901 (2009).
- [36] C. Brun, F. Ladiau, D. L'Hote, G. Biroli, and J-P. Bouchaud, Phys. Rev. Lett. **109**, 175702 (2012).
- [37] S. Capaccioli, G. Ruocco, and F. Zamponi, J. Chem. Phys. B **113**, 10652 (2008).